

# Predicted Solar Cycle Twenty-two 10.7 cm Flux and Satellite Orbit Decay<sup>1</sup>

W. Kent Tobiska,<sup>2</sup> Robert D. Culp,<sup>3</sup> and Charles A. Barth<sup>4</sup>

## Abstract

This study develops an empirical model of the 10.7 cm solar flux ( $F_{10.7}$ ) through solar cycle twenty-two as it relates to the problem of a low-Earth orbiting satellite and its orbit decay. A comparison between the predicted orbit decay using the model and the first thirty-seven months of actual altitude of the Solar Mesosphere Explorer (SME) satellite is conducted. The predicted orbit semimajor axis is solved as a function of atmospheric density using a modified Jacchia 1971 atmospheric model (J71). J71 densities vary based on the empirically modeled  $F_{10.7}$  of solar cycle twenty-two. The derivation of the orbit radius,  $r$ , related to atmospheric mass density,  $\rho$ , is outlined, as are the simplifications made in this study for atmospheric density modeling. The  $F_{10.7}$  model for solar cycle twenty-two is then detailed with a comparison to one other model. Finally, the results of the predicted SME orbit decay are evaluated against the actual orbit decay.

## Introduction

SME is a NASA Explorer series satellite operated by the Laboratory for Atmospheric and Space Physics (LASP) at the University of Colorado (CU) in Boulder. The primary scientific mission of SME is to provide a comprehensive study of mesospheric ozone creation and depletion [1]. SME was launched from the Western Test Range into a polar, Sun-synchronous three pm ascending node orbit on October 6, 1981. The nearly circular orbit had an initial eccentricity of 0.0032 with an altitude near 540 km. The 97.5 degree inclination allows for orbit precession of approximately one degree per day. Science and engineering data is received daily at the Project Operations Control Center located at CU. This site houses the SME mission control, mission planning, and data analysis teams.

<sup>1</sup>Contents were presented at AIAA/AAS 1986 Astrodynamics Conference as Paper No. 86-2223CP.

<sup>2</sup>University of Colorado, Boulder, CO 80309.

<sup>3</sup>Aerospace Engineering Sciences, University of Colorado, Boulder, CO 80309.

<sup>4</sup>Laboratory for Atmospheric and Space Physics, University of Colorado, Boulder, CO 80309.

In the last three decades, there has been extensive work conducted on the problem of satellite orbit perturbations. Both analytic and numerical approaches have shed new light on the behavior of low-Earth orbiting satellites. Liu [2] has outlined a number of these studies which use either analytic or semi-analytic methods to describe satellite behavior.

In predicting orbit perturbations due to atmospheric drag, the predominant uncertainty is the atmospheric density, which varies with the temperature of the atmosphere. Much effort has been placed on developing accurate empirical atmospheric density models since the late 1950's. Most notably, Harris and Priester [3] developed a linear relation between  $F_{10.7}$  and minimum and maximum exospheric temperatures which led to the COSPAR International Reference Atmosphere (CIRA 65) [4]. Jacchia [5] further developed the upper atmosphere model by including solar, geomagnetic, temporal, and geographic parameters represented by empirical equations. His work (termed J71) was adopted as the CIRA 72 model atmosphere. Hedin, et al. used mass spectrometer data from five satellites and incoherent scatter radar measurements from four ground stations to initially develop a thermospheric temperature and density model in which the quantities were empirically represented by expansions in terms of spherical harmonics [6, 7]. Hedin's most recent work [8], MSIS 86, is a candidate for the CIRA 86 model atmosphere. Hedin recently outlined the historical development as well as the advantages and disadvantages of model atmospheres [9].

An important parameter for these models is the variation in  $F_{10.7}$  which is used as an observable indicator of solar extreme ultraviolet (EUV) flux. This flux, consisting of wavelengths shorter than 1031 Å down to the x-rays, is absorbed in the thermosphere by atomic oxygen, O, and molecular nitrogen and oxygen, N<sub>2</sub> and O<sub>2</sub>. The result is atmospheric heating.  $F_{10.7}$  daily variations have been systematically reported since 1947 [10] and now provide a record spanning nearly four solar cycles [11]. Modeling of  $F_{10.7}$  has been of great interest to the astronomical and atmospheric science communities. Predictions have been improved in recent years since Jacchia [12] and others found that thermospheric densities generally vary as  $F_{10.7}$ . Hinteregger and Fukui [13] provided a two-variable formulation for  $F_{10.7}$  based on statistical correlations with Atmospheric Explorer E (AE-E) EUV data. This followed work by Ohl and Ohl [14] and Sargent [15], and by Schatten, et al. [16] and Brown [17] who predicted the sunspot ( $R_z$ ) activity for solar cycle twenty-one using the analyses of secular variations (or the "Ohl-Sargent method") and solar dynamo theory, respectively. Schatten and Hedin [18] predicted the  $R_z$  and  $F_{10.7}$  for solar cycle twenty-two using the dynamo theory, Sargent [19] predicted the length and amplitude of cycle twenty-two  $R_z$  using an observation of even/odd cycle characteristics, and Smith [20] outlined a solar activity prediction technique based on Lagrangian smoothing combined with a linear regression of solar cycle datasets.

This paper presents the results of an extended empirical model of predicted  $F_{10.7}$  based upon Sargent's  $R_z$  work [19] and is combined with King-Hele's [21] analytic orbit determination method in simplified form. The  $F_{10.7}$  is then linked with a modified J71 model atmosphere to determine the predicted orbit decay of SME, creating an ephemeris until estimated reentry in the mid-1990's.

Assumptions simplifying this problem include presuming a circular SME orbit, using a spherical planet and non-rotating, non-mixing, three constituent atmosphere

(Table 1 and Fig. 1), neglecting gravitational field perturbations, assuming constant orbit elements of  $\Omega$ ,  $\omega$ ,  $\epsilon$ ,  $i$  while the semimajor axis,  $a$ , changes secularly due to drag (Table 2), neglecting  $F_{10.7}$  variations due to solar rotation, accepting a strong correlation between  $F_{10.7}$  and atmospheric density, and holding SME's area constant.

Table 1 from Banks and Kockarts [22] lists the reference concentrations of O, N<sub>2</sub>, and O<sub>2</sub> which are the dominant species at 120 km. Figure 1 verifies the three constituent J71 model atmosphere. The profiles are based on a moderate solar activity index of  $F_{10.7} = 130$ . SME's derived density for thirty-three months is overplotted, corresponding to a range of high to low solar activity (1982-1984). Table 2 outlines

TABLE 1. Thermospheric Composition at 120 km<sup>5</sup>

Species	Atomic/Molecular Wgt (AMU)	Number Density (m <sup>-3</sup> ) at 120 km
O	16	$7.6 \times 10^{16}$
N <sub>2</sub>	28	$5.8 \times 10^{17}$
O <sub>2</sub>	32	$1.2 \times 10^{17}$

<sup>5</sup>From Banks and Kockarts [22].

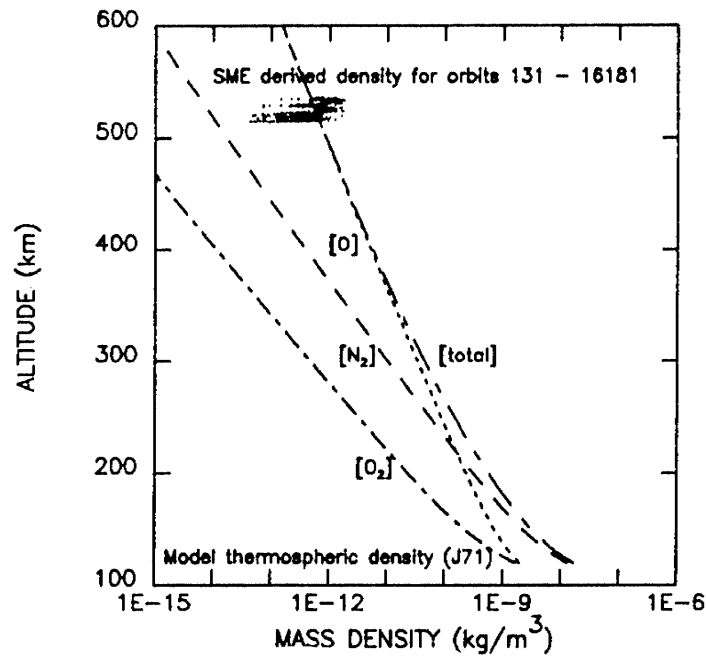


FIG. 1. Three constituent J71 model atmosphere above 120 km for moderate solar activity of  $F_{10.7} = 130$ . SME derived density is overplotted for orbits 131-16181 (thirty-three months). The minimum data points correspond to  $F_{10.7} = 75$  in late 1984 while the maximum data points reflect  $F_{10.7} = 289$  in early 1982.

TABLE 2. Satellite Perturbations for Orbits Below 600 km<sup>6</sup>

Perturbing Source	Secular		Periodic	
	large	small	moderate	small
Earth Grav. Field	$\Omega, \omega$	—	$\varepsilon$	$i, \Omega, \omega$
Atmosphere	$a, \varepsilon$	$i$	—	$\Omega, \omega$
Lunar-Solar	—	—	—	$a, \varepsilon, i, \Omega, \omega$

<sup>6</sup>From King-Hele [21].

King-Hele's analysis of satellite perturbations. While the Earth gravitational field will secularly perturb the ascending node,  $\Omega$ , and the argument of periapsis,  $\omega$ , these variables are not used in determining the radius,  $r$ , as a function of density in this study. Secular changes in eccentricity,  $\varepsilon$ , and inclination,  $i$ , from atmospheric perturbations become very small when  $\varepsilon \approx 0$  and for an  $i$  such as SME's. Only the large, secular perturbation of the semimajor axis,  $a$ , by the atmosphere is considered in this study.

### SME Orbit Model

#### *Radius as a Function of Density*

Aerodynamic drag is described as

$$F_d = \frac{1}{2} C_d A \rho v^2 \quad (1)$$

where  $C_d$  is the drag coefficient,  $A$  is the satellite area,  $\rho$  is the atmospheric density, and  $v$  is the satellite velocity relative to the atmosphere. It can be shown that, assuming a circular orbit where  $a = r$ , the work done by the atmosphere on a satellite affects the rate change of its orbit radius,  $r$ , and can be written as

$$\dot{r} = \frac{C_d A \rho v^3 2r^2}{2\mu m} \quad (2)$$

where  $\mu$  is the Earth's gravitational constant and  $m$  is the satellite mass. By substituting the time derivative of the orbit period, the radius as a function of density is

$$r = \frac{1}{3\pi\rho(A/m)C_d} \dot{P} \quad (3)$$

Using a constant time interval,  $dt$ , this equation can be readily integrated on the computer, solving for the altitude as a function of a modeled atmospheric density.

#### *Atmospheric Density Modeling*

Accepting atmosphere modeling [23] describes the density equation of a  $j$ th constituent, based on the Ideal Gas Law of  $p = nkT$  and gravity,  $g(z)$ , as a function of altitude,  $z$ . The barometric law is derived from the hydrostatic equation and may be

written as the density equation

$$n_j(z) = n_j(z_0) \exp\left(-\frac{dz}{H_j(z)}\right) \quad (4)$$

The constituent altitude dependent density scale height is  $H_j(z) = kT(z)/m_j g(z)$ .  $dz = z - z_0$ ,  $n_j(z_0)$  is a reference altitude constituent concentration,  $k$  is Boltzman's constant,  $T(z)$  is temperature in Kelvin for an altitude, and  $m_j$  is a constituent mass. The mass density of the thermosphere,  $\rho_j$ , is  $\rho_j(z) = n_j(z)m_j$ .

For altitudes above 120 km, the atmosphere is not well mixed. This is due to diffusive separation and it requires each constituent's scale height to be considered separately. Hence, the density at an altitude of each of the three principal neutral thermosphere components is determined individually and summed to give the total modeled thermospheric density,  $\rho(z)$ . Its variation over a solar cycle is primarily due to the variation in  $T(z)$ .

*Average Exospheric Temperature*

Following the derivation of Bates [24], the thermospheric temperature at an altitude is defined as

$$T(z) = T_\infty - (T_\infty - T_0)e^{-\sigma(z-z_0)} \quad (5)$$

where the parameter  $\sigma$  is

$$\sigma = \frac{\left. \frac{dT}{dz} \right|_{z=z_0}}{T_\infty - T_0} \quad (6)$$

and is evaluated at a reference altitude  $z = z_0$ .  $T_\infty$  is the exospheric temperature and  $T_0$  is the reference altitude temperature. A simplified version of Jacchia's empirical equation, using a three solar rotation average of daily  $F_{10.7}$ , is substituted for the nighttime minimum exospheric temperature, giving

$$T_\infty = 379 + 3.24(\overline{F}_{10.7}) \quad (7)$$

The J71 model is further modified to account for an average of both night minimum and day maximum temperatures which a low-Earth orbiting satellite experiences during the course of one orbit. Figure 2 shows a graphical representation of a satellite orbit in an atmosphere with diurnal temperature variations. An average exospheric temperature can be derived [25] by rewriting  $T_\infty$  as

$$\overline{T}_\infty = \frac{1}{\pi} \int_0^\pi f(\theta) d\theta \quad (8)$$

where  $f(\theta) = A(\sin B\theta + 1)$  is an idealized, continuous function of diurnal temperatures over an orbit path for an arbitrary  $A$  and  $B$ . Using the boundary conditions of  $0 \leq \theta \leq \pi$  for a half orbit,  $A = 379 + 3.24(\overline{F}_{10.7})$  which is the  $T_\infty$  nighttime minimum value, and  $B = 0.09699$  which allows  $T_\infty$  to attain a maximum day value. By integrating and substituting,  $\overline{T}_\infty$  can be written as

$$\overline{T}_\infty = 1.15(379 + 3.24\overline{F}_{10.7}) \quad (9)$$

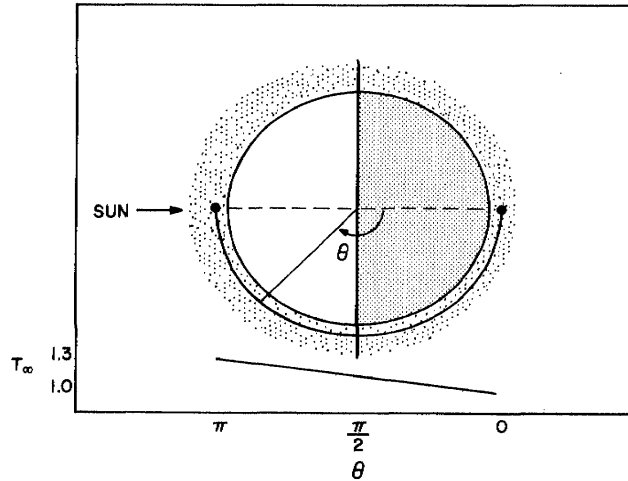


FIG. 2. Graphical representation of one-half a satellite orbit in an atmosphere with diurnal temperature variations. The bottom section demonstrates the approximate range of values of  $T_\infty$  from J71 for a maximum near the projection of the sun line to the minimum 180 degrees away in the atmosphere.

This modified J71 equation is used to determine exospheric temperature as well as the temperature and density at a given thermospheric altitude where  $T_\infty = \bar{T}_\infty$  in equation (5).

#### Iterative Solution of Radius, $r$

The orbit period rate change,  $\dot{P}$ , can be rewritten as a function of both density and the previous value of the orbit radius. If  $r_i = r_{i-1} + \delta r$ , then  $r_{i-1}$  is the previous orbit radius and  $\delta r$  is considered negligible in this problem for one orbit. Hence,

$$\dot{P}_i = 3\pi r_{i-1} \frac{A}{m} C_d \rho_i \quad (10)$$

$\rho_i$  is the modeled total mass density assumed averaged and constant for an orbit. The new radius is calculated as

$$r_i = \left[ \frac{\sqrt{\mu} P_i}{2\pi} \right]^{2/3} \quad (11)$$

where the new period of the satellite is calculated from  $P_i = P_{i-1} + \delta P_i$  and  $P_{i-1}$  is the previous orbit period.  $\delta P_i = \dot{P}_i dt$  where  $dt$  is a fixed time interval.

#### 10.7 cm Flux Prediction

The principal items needed for the prediction of temperatures and thus thermospheric densities using  $F_{10.7}$  over the next solar cycle include a good estimate of the amplitude of cycle twenty-two and good estimates of the location for the minimum and maximum of cycle twenty-two as well as the minimum of cycle twenty-one. Sargent [19] of the Space Environment Laboratory at NOAA developed a forecast for the

sunspot numbers,  $R_z$ , during cycle twenty-two. A method of translating the sunspot numbers to  $\bar{F}_{10.7}$  is given by Euler and Holland [26]

$$\bar{F}_{10.7} = 49.4 + 0.97\bar{R} + 17.6e^{-0.035\bar{R}} \tag{12}$$

where  $\bar{R}$  is the recorded smoothed sunspot data.

Several points should be raised about solar cycle activity before proposing an empirical model. Sargent suggests that solar cycles can be numbered in even-odd pairs, with the characteristic that the preceding even cycle generally predicts the maximum of the following odd cycle. After observing the last six even-odd pairs, the slopes before and after maximum solar activity of the even cycle tend to predict the slopes of the succeeding odd cycle. Figure 3 illustrates this.

As noted by Sargent, an important difference between the even and odd cycles in a pair is that the even cycle has its top "chopped off." Two pieces of information come from Fig. 3. First, the sets of even-odd cycles (from ten to twenty-one) average 10.2 to 11.7 years between minimums, with a total of about twenty-two years for a pair (Fig. 4). Second, the average ratio of the odd cycle to the even cycle in the data is 1.44 (Table 3). This information makes it easier to predict cycle twenty-three from cycle twenty-two. However, there is not a good relationship like this to predict the amplitude of an even cycle from the preceding odd cycle, as in the case of predicting cycle twenty-two.

*Solar Cycle Amplitudes*

The average maximum of the sunspot cycles since 1848 is 117.5  $R_z$  which translates to  $F_{10.7} = 158$ . This can be used as one possible value for the maximum of cycle twenty-two.

In observing the amplitudes of solar cycles since 1848, (Fig. 5) the phenomenon of the Gleissburg cycle has been suggested. What appears in the data over the last 140 years is a general indication of an eighty to ninety year cycle. Beginning with the

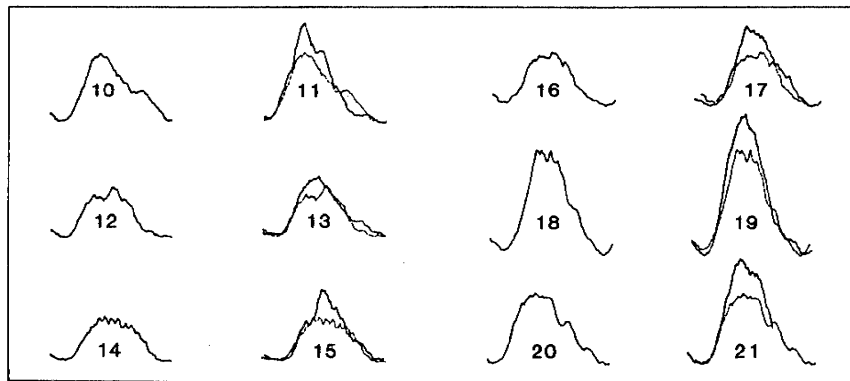


FIG. 3. Even-odd sunspot pairs for cycles ten through twenty-one. The preceding even cycle is matched with each odd cycle, showing a comparison between ascending and descending slopes. From Sargent [19].

TABLE 3. Even-odd  $R_z$  Cycle Maximums and Pair Ratios<sup>7</sup>

Cycle	Maximum	Ratio
10	97.9	
11	140.5	1.44
12	74.6	
13	87.9	1.18
14	64.2	
15	105.4	1.64
16	78.1	
17	119.2	1.53
18	151.8	
19	201.3	1.33
20	110.6	
21	164.5	1.49
		average = 1.44

<sup>7</sup>From Sargent [19].

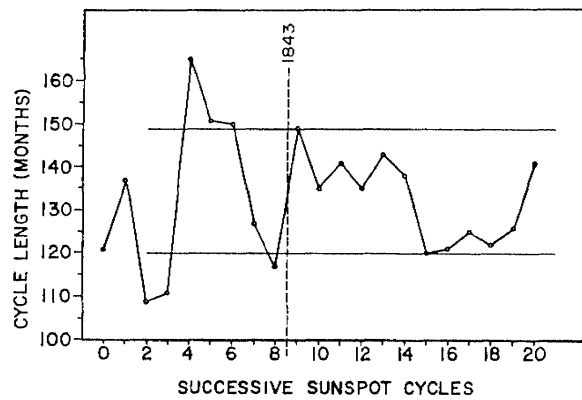


FIG. 4. Successive sunspot cycles plotted with cycle length in months. The two lines show the limiting cases of post-1848 cycles of 150 and 120 months. After 1848, there appear to be series of long length and short length cycles. The averages of these are 11.7 years and 10.2 years from minimum to minimum, respectively. From Sargent [19].

present cycle around the turn of the century, there is an increase in the solar maximums to a peak level in midcentury. From the data, it appears that cycle twenty-two is nearing the end of a Gleissburg cycle. For this reason, the maximum of cycle twenty-two (an even, low amplitude solar cycle) should be lower than the peak of cycle twenty, the last low amplitude cycle.

Referring to cycle twenty, it had a maximum of 110.6  $R_z$  or  $F_{10.7} = 152$ . Accepting this, it means the prediction of  $F_{10.7} = 158$  is going the wrong way if the Gleissburg cycle is valid. In rethinking the data, Sargent suggests that a better value for the

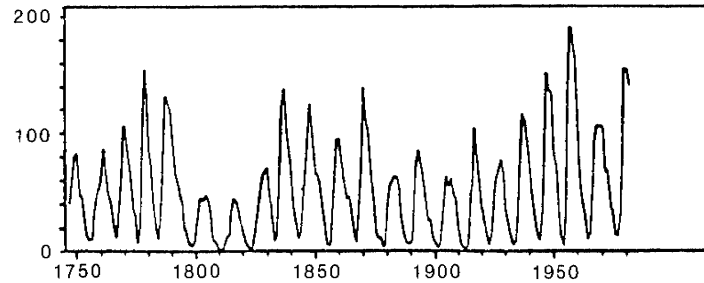


FIG. 5. Annual average sunspot numbers from 1750 to 1980 showing the possible Gleissburg 80–90 year cycle. From Sargent [19].

maximum  $R_z$  of cycle twenty-two might be between 90 and 100, which translates to  $F_{10.7} \approx 135 - 143$ . This allows for a decrease in the solar maximum according to the Gleissburg cycle pattern and would still be well within range of the average  $R_z$  values over modern times. This assumption leads to an estimated average maximum value of  $F_{10.7} = 140$ . Sargent also points out that in the modern era,  $R_z$  of 96.2 ( $F_{10.7} = 140$ ) is the average for the even cycle maximum amplitudes, giving more confidence in selecting that value.

Sargent does not make a forecast for the minimum of cycle twenty-one. In arriving at a best guess of  $F_{10.7} = 66$ , the values of the minimums for the last five cycles were averaged. The minimum  $F_{10.7}$  for cycle twenty-one should be similar.

#### *Solar Cycle Length*

The present study's predicted location of the minimum of cycle twenty-one ranges from June 1986 to November 1988, with a most likely date in February 1988. This point in the cycle reflects the general trend over the past 140 years where one average time between minimums is 140 months. Sargent points out that there are really two sets of data (and thus averages) for sunspot cycle lengths (Fig. 4). One set has lengths of 140 or 150 months while the other set has lengths in the range of 120 or 130 months. Each set seems to be organized in a series. Sargent notes that the last series was of short length, with cycle twenty having just entered the long length range. Since there is no indication in the data that the cycles successively jump from long to short lengths in alternating cycles, a cycle twenty-one length could be expected somewhere near that of cycle twenty. The average length for the longer series of cycles is around 140 months, which is the same range for the cycle twenty length. In fact, this is not much higher than the overall cycle length average of 133 months. For this study, an intermediate value between Sargent's 140 months and the overall average of 133 months was selected, giving a cycle twenty-one length of 138 months. This weights the cycle length using Sargent's analysis and places the solar minimum in December 1987.

Figure 6 is the plot of predicted  $F_{10.7}$  of cycle twenty-two with the equations for the solid, best estimate curve given in Table 4. The maximum of cycle twenty-two occurs over a relatively large period, approximately twenty-one months. This plateau of average monthly  $F_{10.7}$  values follows the trend over the last four even solar cycles. The